AJNR

Can 3T MR Angiography Replace DSA for the Identification of Arteries Feeding Intracranial Meningiomas?

H. Uetani, M. Akter, T. Hirai, Y. Shigematsu, M. Kitajima, Y. Kai, S. Yano, H. Nakamura, K. Makino, M. Azuma, R. Murakami and Y. Yamashita

AJNR Am J Neuroradiol published online 18 October 2012
http://www.ajnr.org/content/early/2012/11/08/ajnr.A3284

Published November 8, 2012 as 10.3174/ajnr.A3284

Can 3T MR Angiography Replace DSA for the Identification of Arteries Feeding Intracranial Meningiomas?

H. Uetani, M. Akter, T. Hirai, Y. Shigematsu, M. Kitajima, Y. Kai, S. Yano, H. Nakamura, K. Makino, M. Azuma, R. Murakami, and Y. Yamashita

ABSTRACT

BACKGROUND AND PURPOSE: For identifying the arterial feeders of meningiomas, the usefulness of 3D TOF MRA at 3T has not been systematically investigated. This study was intended to assess whether unenhanced 3D TOF MRA at 3T can replace DSA for the identification of arteries feeding intracranial meningiomas and whether it is useful for assessing their dural attachment.

MATERIALS AND METHODS: Twenty-one consecutive patients with intracranial meningiomas (18 women, 3 men; aged 42–77 years, mean 57 years) underwent DSA, conventional MR imaging, and 3D TOF MRA. Two neuroradiologists independently evaluated the primary and secondary feeders of each tumor on maximum-intensity-projection and source MRA images. They also identified the location of dural attachments based on information from MR imaging/MRA images. Interobserver and intermodality agreement was determined by calculating the κ coefficient.

RESULTS: For the identification of primary and secondary feeders on MRA images, interobserver agreement was very good ($\kappa = 0.83$; 95% CI, 0.66–1.00) and moderate ($\kappa = 0.58$; 95% CI, 0.34–0.82) and intermodality agreement (consensus reading of MRA versus DSA findings) was excellent ($\kappa = 0.94$; 95% CI, 0.84–1.00) and good ($\kappa = 0.72$; 95% CI, 0.51–0.93), respectively. With respect to the dural attachment of meningiomas, interobserver agreement was very good ($\kappa = 0.95$; 95% CI, 0.84–1.00). The agreement in the diagnosis between MR imaging/MRA and surgery was excellent ($\kappa = 1.00$).

CONCLUSIONS: Unenhanced 3D TOF MRA at 3T cannot at present supplant DSA for the identification of the feeding arteries of intracranial meningiomas. This information may be useful for evaluating their dural attachment.

ABBREVIATIONS: CI = confidence interval; MIP = maximum intensity projection; MOTSA = multiple overlapping thin slab acquisitions; MPR = multiplanar reconstruction; NSA = number of signal-intensity acquisitions; TOF = time-of-flight.

Meningiomas are the most frequently diagnosed primary brain tumors, and account for approximately one-third of these tumors.[1] They tend to be hypervascular and are fed by arteries attached to the dura. In patients with meningioma, tumor embolization is considered a useful preoperative adjuvant therapy to mitigate blood loss during subsequent surgical resection.[2] To determine the need for preoperative embolization, one must understand the tumor vasculature. For the selection of the optimal surgical approach to meningiomas, the precise anatomic location of the dural attachment must be understood, and the critical feeding arteries must be localized early.[3,4]

Received April 12, 2012; accepted after revision June 19.

From the Departments of Diagnostic Radiology (H.U., M. Akter, T.H., Y.S., M.K., M. Azuma, Y.Y.), Neurosurgery (Y.K., S.Y., H.N., K.M.), and Medical Imaging (R.M.), Graduate School of Medical Sciences, Kumamoto University, Kumamoto, Japan.

Please send correspondence to Toshinori Hirai, Department of Diagnostic Radiology, Graduate School of Medical Sciences, Kumamoto University, 1-1-1 Honjo, Kumamoto 860-8556 Japan; e-mail: t-hirai@kumamoto-u.ac.jp

http://dx.doi.org/10.3174/ajnr.A3284

Intra-arterial DSA, the reference standard for assessing the vasculature of meningiomas, plays a role in planning the embolization of large tumors and tumors whose blood supply is inaccessible (eg, those of the base of the skull).[5] The inherently high spatial and temporal resolution of DSA facilitates the identification of the feeding arteries and tumor vascularity. Because DSA is invasive, exposes the patient to radiation, requires the injection of iodinated contrast material, and does not show anatomic relationship with brain structures, however, a noninvasive method is needed for the accurate diagnosis of these tumors and their preinterventional and presurgical evaluation.

Unenhanced 3D TOF MRA is a safe, less expensive, widely used, and noninvasive imaging technique. Source images from 3D TOF MRA yield both flow and anatomic information with high spatial resolution.[6,7] As the quality and spatial resolution of 3D TOF MRA is improved on 3T MR units,[8-10] 3D TOF MRA at 3T can be expected to provide precise information on the vessels feeding meningiomas. To our knowledge, there are no comparative studies on 3D TOF MRA at 3T and DSA to assess their utility for identifying

Table 1: Summary of patients and intracranial meningiomas

Case No.	Age	Sex	Clinical Manifestation	Size[a] (mm)	Primary Feeders	Secondary Feeders	Location of Dural Attachment[b]
1	48	F	Hemiparesis	77	MMA	–	Cerebral convexity
2	65	F	Headache	54	MCA	MMA	Cerebral convexity
3	75	F	Headache	59	MMA	OphA	Cerebral convexity
4	67	F	Speech dist.	48	MMA	MCA	Cerebral convexity
5	68	F	Gait dist.	31	MMA	ACA	Falx
6	67	F	Speech dist.	67	MMA	OA	Parasagittal
7	77	F	Hemiparesis	40	MMA	ACA	Parasagittal
8	59	F	Visual dist.	65	ILT	AMA	Sphenoid ridge
9	66	M	Headache	54	OphA	MCA	Sphenoid ridge
10	55	F	Visual dist.	73	OphA	MHT	Sphenoid ridge
11	47	F	Hemiparesis	46	OphA	MHT	Sphenoid ridge
12	43	F	Visual dist.	62	OphA	MMA	Sphenoid ridge
13	62	F	Visual dist.	50	AMA	MHT	Anterior clinoidal
14	71	F	Visual dist.	50	ILT	MHT	Central skull base
15	42	M	Headache	73	MHT	MMA	Middle cranial fossa
16	49	F	Headache	91	MHT	MMA	Tentorial
17	50	F	Trigeminal n.	21	MHT	–	Petroclival
18	59	F	Gait dist.	41	ILT	–	Petroclival
19	44	F	Headache	43	OA	–	T-S sinus junction
20	49	M	Headache	24	AICA	APhA	Cerebellopontine angle
21	44	F	Gait dist.	54	OA	MMA	Cerebellar convexity

Note:—F indicates female; M, male; Speech dist., speech disturbance; Visual dist., visual disturbance; Trigeminal n., trigeminal neuralgia; Gait dist., gait disturbance; MMA, middle meningeal artery; AMA, accessory meningeal artery; APhA, ascending pharyngeal artery; OA, occipital artery; OphA, ophthalmic artery; ILT, inferolateral trunk; MHT, meningohypophyseal trunk; MCA, middle cerebral artery; ACA, anterior cerebral artery; AICA, anterior inferior cerebellar artery; T-S sinus junction, transverse-sigmoid sinus junction; –, None.

[a] Maximum diameter of the tumor.

[b] Final diagnosis of dural attachment was determined by surgical findings. When total tumor resection was not obtained, DSA findings were also used for determining the dural attachment of meningiomas.

the arterial feeders of meningiomas. Here we tested our hypothesis that unenhanced 3D TOF MRA at 3T can replace DSA for the identification of the feeders of intracranial meningiomas and that it is useful for assessing their dural attachment.

MATERIALS AND METHODS

Patients

This study was approved by our institutional review board. Informed consent for imaging studies was obtained from all patients or their legal representatives. Our prospective study included 21 consecutive patients whose initial diagnosis was intracranial meningioma (18 women, 3 men; age range 42–77 years, mean age 57 years ± 11) and who underwent preoperative DSA and 3D TOF MRA at 3T. The interval between DSA and 3D TOF MRA ranged from 2 to 30 days (mean 11 days).

Of the 21 meningiomas, 15 were supratentorial, 5 were infratentorial, and 1 was supra- and infratentorial. The presenting symptoms were headache in 7 patients, visual disturbance in 5, hemiparesis in 3, gait disturbance in 3, speech disturbance in 2, and trigeminal neuralgia in 1 (Table 1).

MR Imaging and MRA

All MR imaging studies were done on a 3T scanner (Achieva 3T; Philips Medical Systems, Best, the Netherlands) using 8-channel head coils. The imaging sequences included 3-plane scout localizers, axial spin-echo T1-weighted (TR/TE/NSA 450 ms/10 ms/1, matrix 320 × 320), turbo spin-echo T2-weighted (TR/TE/NSA 4060 ms/80 ms/1, turbo factor 9, matrix 512 × 512), FLAIR (TR/TE/NSA/TI 9000 ms/120 ms/1/2500 ms, turbo factor 15, matrix 352 × 352), 3D TOF MRA, and postcontrast T1-weighted and 3D turbo field echo (TR/TE/NSA 450 ms/10 ms/1, matrix 320 × 320) images. FOV was 23 cm on all conventional MR images.

The volume for 3D TOF MRA by using MOTSA was localized on a sagittal scout image. The parameters were TR/TE/NSA 20 ms/3.5 ms/1, flip angle 20°, FOV 20 × 20 cm, matrix 512 × 512, 5 slabs, voxel size 0.39 × 0.39 × 1.0 mm (reconstructed voxel size 0.25 × 0.25 × 0.5 mm), parallel imaging factor 2, and acquisition time 4 minutes 48 seconds. Cephalad saturation pulses were applied to eliminate venous blood signals. When a meningioma was located at the top of the head, another 3D TOF MRA slab was rostrally added by using the same parameters. MIP and partial MIP techniques were used for the 3D display of MRA images. Coronal and sagittal images acquired with the MPR method were also reconstructed for the observers' interpretation.

DSA Technique

After catheterization of the internal and external carotid and vertebral arteries via a femoral artery approach, diagnostic biplanar intra-arterial DSA (Allura Xper FD; Philips Medical Systems) was performed by a trained neuroradiologist and/or a neurosurgeon. Images were obtained with a 2048 × 2048 matrix and a 17-cm FOV. The temporal resolution of the images was 3 frames/s. For each projection we manually injected a 6- to 10-mL bolus of an undiluted iodinated contrast material with an iodine concentration of 300 mg/mL (Iopamidol, Iopamiron 300; Bayer-Schering, Berlin, Germany).

Image Analysis

Two independent readers (Y.K. and T.H., with 23 and 21 years of experience in neuroangiography, respectively) qualitatively evaluated the entire series of DSA images on a PACS workstation.

Disagreements were resolved by consensus. Two other readers (M.K. and Y.S., with 19 and 18 years of experience in diagnostic neuro-MR imaging, respectively) blinded to the clinical and DSA results, independently evaluated the 3D TOF MRA data on a PACS workstation. In each case, the 3D, MPR, and MRA source images and conventional MR imaging data were displayed with all regions visible. The software allowed the enlargement of regions of special interest in any given spatial orientation.

DSA and 3D TOF MRA data were assessed to identify primary and secondary feeders. Tumor feeders were defined as arterial branches continuing to or entering the tumor that originated at the external carotid artery (eg, the middle meningeal, accessory meningeal, ascending pharyngeal, or occipital artery); the internal carotid artery (eg, the ophthalmic artery, inferolateral trunk, meningohypophyseal trunk); the middle cerebral, anterior cerebral, posterior cerebral, or cerebellar artery (eg, the superior, anterior inferior, or posterior inferior cerebellar artery); or other arteries. When no feeders were identified, the readers recorded "none." The volume of blood supplied to the tumor was estimated based on the feeder caliber and/or the stain volume on DSA and MRA images. The primary feeder was considered to be the artery that supplied most of the blood to the tumor; the following supplying artery was designated the secondary feeder.

Experienced neurosurgeons who performed or assisted at surgery determined the anatomic location of the dural attachment of each meningioma based on surgical findings. When total tumor resection was not obtained, DSA findings were also used for determining the dural attachment of meningiomas.[11] The 2 readers (M.K. and Y.S.) who were blinded to surgical and DSA results, also independently recorded the location of the dural attachment of each tumor based on MRA and conventional MR imaging studies. The location of the dural attachment was recorded as cerebral convexity, falx, parasagittal, sphenoid ridge, anterior clinoidal, central skull base, anterior cranial fossa, middle cranial fossa, tentorial cerebelli, petroclival, transverse-sigmoid sinus junction, cerebellopontine angle, cerebellar convexity, or other. Final agreements were obtained by consensus. After the blinded study the 2 readers retrospectively and consensually reviewed additional information of 3D TOF MRA compared with conventional MR images.

Statistical Analysis

The levels of interobserver agreement (between readers 1 and 2 for DSA and MRA images) and intermodality agreement (between consensus readings of MRA and DSA images) with respect to primary and secondary arterial feeders were determined by calculating the κ coefficient ($\kappa < 0.20$ = poor; $\kappa = 0.21–0.40$, fair; $\kappa = 0.41–0.60$, moderate; $\kappa = 0.61–0.80$, good; $\kappa = 0.81–0.90$, very good; and $\kappa > 0.90$, excellent agreement).

With regard to the dural attachment of the meningiomas, interobserver agreement between the 2 readers of MRA/MR imaging studies, and the agreement between the diagnosis from consensus readings of MRA/MR imaging and the final diagnosis based on surgery/DSA were determined by calculating the κ coefficient.

We also recorded the exact number and percentage of times when the results from the 2 readers, the 2 modalities, and the MRA/MR imaging and final diagnosis were in exact agreement, including the 95% CI. A statistical package, MedCalc for Windows (MedCalc Software, Mariakerke, Belgium), was used for all analyses.

RESULTS

The primary and secondary meningioma feeders identified on DSA images are shown in Table 1. At qualitative evaluation of DSA, interobserver agreement was excellent for primary and secondary feeders ($\kappa = 1.0$; 95% CI, 1.0 −1.0). Table 2 is a summary of the DSA and 3D TOF MRA findings on the 21 meningiomas.

On DSA images, 6 meningiomas were supplied primarily by the middle meningeal artery, 4 by the ophthalmic artery, 3 each by the inferolateral trunk and meningohypophyseal trunk, 2 by the ophthalmic artery, and 1 each by the middle cerebral artery, accessory meningeal artery, and anterior inferior cerebellar artery (Table 1). In the analysis of the primary arterial feeders, the 2 readers reviewing MRA images agreed in 18 of 21 studies (86%); interobserver agreement was recorded as very good ($\kappa = 0.83$; 95% CI, 0.66–1.00; Figs 1 and 2). In 20 of 21 studies (95%), the MRA (consensus reading) and DSA findings of the 2 readers coincided with respect to the primary arterial feeders. Intermodality agreement (consensus reading of MRA versus DSA findings) was excellent ($\kappa = 0.94$; 95% CI, 0.84–1.00; Table 2).

The secondary feeders on DSA images were the middle meningeal artery in 5 meningiomas, the meningohypophyseal trunk in 4, the anterior cerebral artery in 2, the middle cerebral artery in

Table 2: Interobserver and intermodality agreement for the identification of primary feeders

	MRA		Interobserver Agreement[a]			Intermodality Agreement[c]
	Reader 1	Reader 2		MRA[b]	DSA	
MMA	6	6		6	6	
AMA	1	1		1	1	
APhA	0	1		1	0	
OA	3	2		2	2	
OphA	4	3		4	4	
ILT	3	3	18 (86%)	3	3	20 (95%)
MHT	2	4	$\kappa = 0.83$	3	3	$\kappa = 0.94$
ACA	0	0	[0.66–1.00]	0	0	[0.84–1.00]
MCA	1	1		1	1	
PCA	0	0		0	0	
SCA	0	0		0	0	
AICA	1	0		0	1	
PICA	0	0		0	0	
Other	0	0		0	0	

Note:—Data are number of meningiomas. Data in parentheses are the percentage of times that results that were concordant, and data in brackets are 95% confidence intervals. MMA indicates middle meningeal artery; AMA, accessory meningeal artery; APhA, ascending pharyngeal artery; OA, occipital artery; OphA, ophthalmic artery; ILT, inferolateral trunk; MHT, meningohypophyseal trunk; MCA, middle cerebral artery; ACA, anterior cerebral artery; PCA, posterior cerebral artery; SCA, superior cerebellar artery; AICA, anterior inferior cerebellar artery; PICA, posterior inferior cerebellar artery.

[a] Agreement of MRA between Reader 1 and Reader 2.

[b] Consensus reading at MRA of Reader 1 and Reader 2.

[c] Agreement between the consensus reading of MRA of Reader 1 and Reader 2 and DSA.

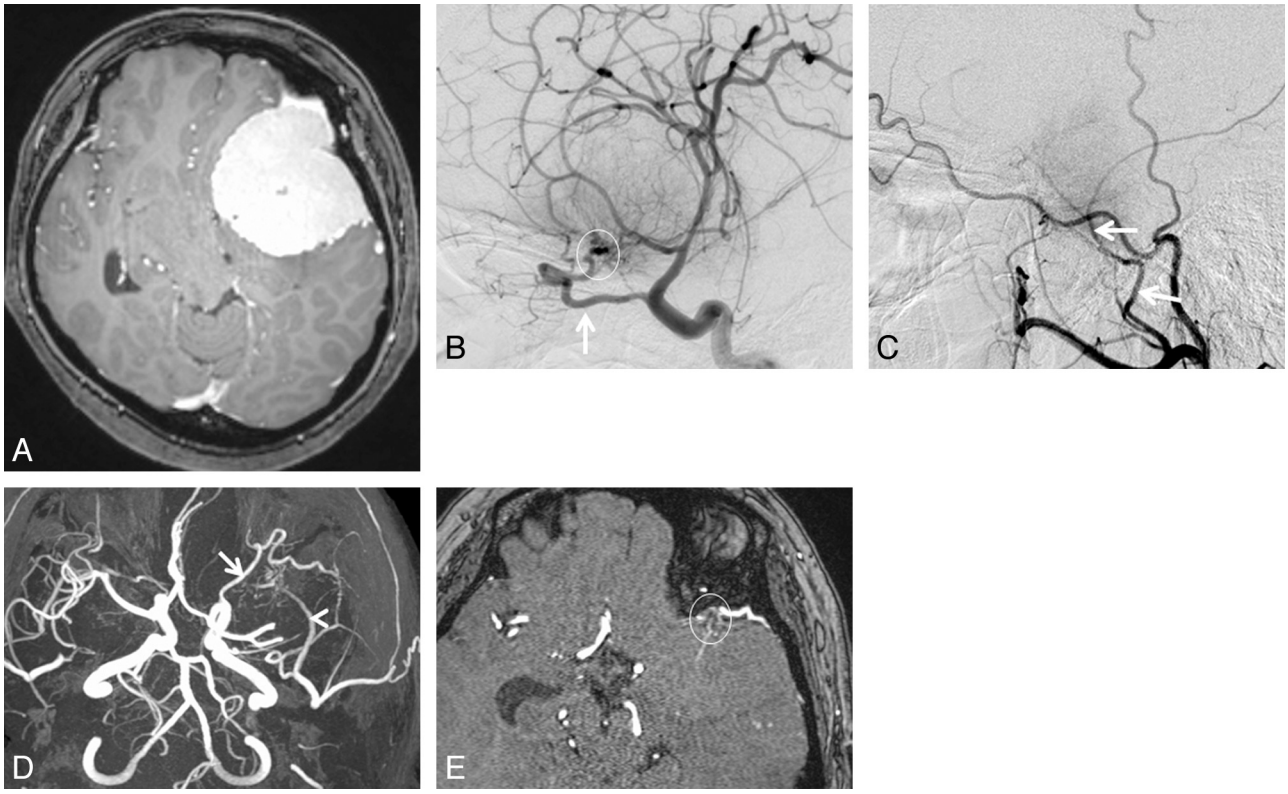

FIG 1. A 43-year-old woman with sphenoid ridge meningioma. *A*, Axial contrast-enhanced 3D turbo field echo image showing a large enhanced mass in the left anterior to middle cranial fossa regions. *B,* DSA (lateral projection from the left internal carotid artery) reveals a tumor fed primarily by the recurrent meningeal artery of the ophthalmic artery (*arrow*). Based on the surgical findings, the dural attachment was the sphenoid ridge (*circle*). *C,* DSA (lateral projection from the left external carotid artery) shows a tumor fed partially by the middle meningeal artery (*arrows*). The right middle meningeal artery was judged to be the secondary feeder. *D,* 3D TOF MRA (axial projection) depicts dilated branches from the left ophthalmic (*arrow*) and middle meningeal arteries (*arrowhead*). *E,* This axial source 3D TOF MRA image shows tumor-feeding branches from the left ophthalmic artery at the left sphenoid ridge (*circle*). Both readers judged that the ophthalmic artery was the primary feeder and that the dural attachment was the left sphenoid ridge.

2, and the ophthalmic artery, accessory meningeal artery, occipital artery, and ascending pharyngeal artery in 1 each; 4 tumors exhibited no secondary feeders (Table 1). In the analysis of the secondary arterial feeders the 2 readers reviewing MRA images agreed in 15 of 21 studies (71%); interobserver agreement was recorded as moderate ($\kappa = 0.58$; 95% CI, 0.34–0.82; Figs 1 and 2). In 16 of 21 studies (76%), the MRA (consensus reading) and DSA findings of the 2 readers coincided with respect to the secondary arterial feeders. Intermodality agreement (consensus reading of MRA versus DSA findings) was good ($\kappa = 0.72$; 95% CI, 0.51–0.93; Table 3).

Based on surgical findings with or without DSA information, dural attachment was to the sphenoid ridge in 5 meningiomas, the cerebral convexity in 4, the parasagittal and petroclival in 2 each, and the falx, anterior clinoidal, central skull base, middle cranial fossa, tentorial, transverse-sigmoid sinus junction, cerebellopontine angle, and cerebellar convexity in 1 each (Table 1). In the diagnosis from reading of 3D TOF MRA and conventional MR images, the 2 readers agreed in 19 of 21 studies (90%), and the interobserver agreement was recorded as very good ($\kappa = 0.95$; 95% CI, 0.84–1.00). The agreement between the diagnosis from consensus readings of MRA/MR imaging and the final diagnosis based on surgery/DSA was excellent ($\kappa = 1.00$; 95% CI, 1.00–1.00; Table 4).

In the retrospective part of this study, dural attachments were identified correctly on conventional MR imaging alone in 13 (62%) of 21 meningiomas (Fig 3). All dural attachments were identified when 3D TOF MRA was added to conventional MR images. In the 8 meningiomas where 3D TOF MRA was useful for the identification of dural attachments, their location included the sphenoid ridge ($n = 4$), and parasagittal, central skull base, tentorial, and transverse-sigmoid sinus junction ($n = 1$ each; Figs 1 and 2).

DISCUSSION

Compared with DSA, unenhanced 3D TOF MRA at 1.5T or less has been reported to be unsatisfactory for the depiction of arterial meningioma feeders.[12,13] We found that unenhanced 3D TOF MRA at 3T is a reliable diagnostic tool for the identification of primary feeders; the agreement with DSA was excellent ($\kappa = 0.94$; 95% CI, 0.84–1.00). We attribute the excellent identification of primary feeders to the combined effect of several factors.

3T TOF MRA benefits from 2 key conditions. The theoretic signal-to-noise ratio at 3T is twice that at 1.5T, allowing for increased spatial resolution. The longer T1 values of tissues at 3T produce better background suppression, additional inflow enhancement, and improved contrast-to-noise ratios.[8-10] In addition, the MRA sequence we used is based on a combination of MOTSA technique and short TE. In general, the sensitivity of MRA is limited because of phase dispersions from turbulence or

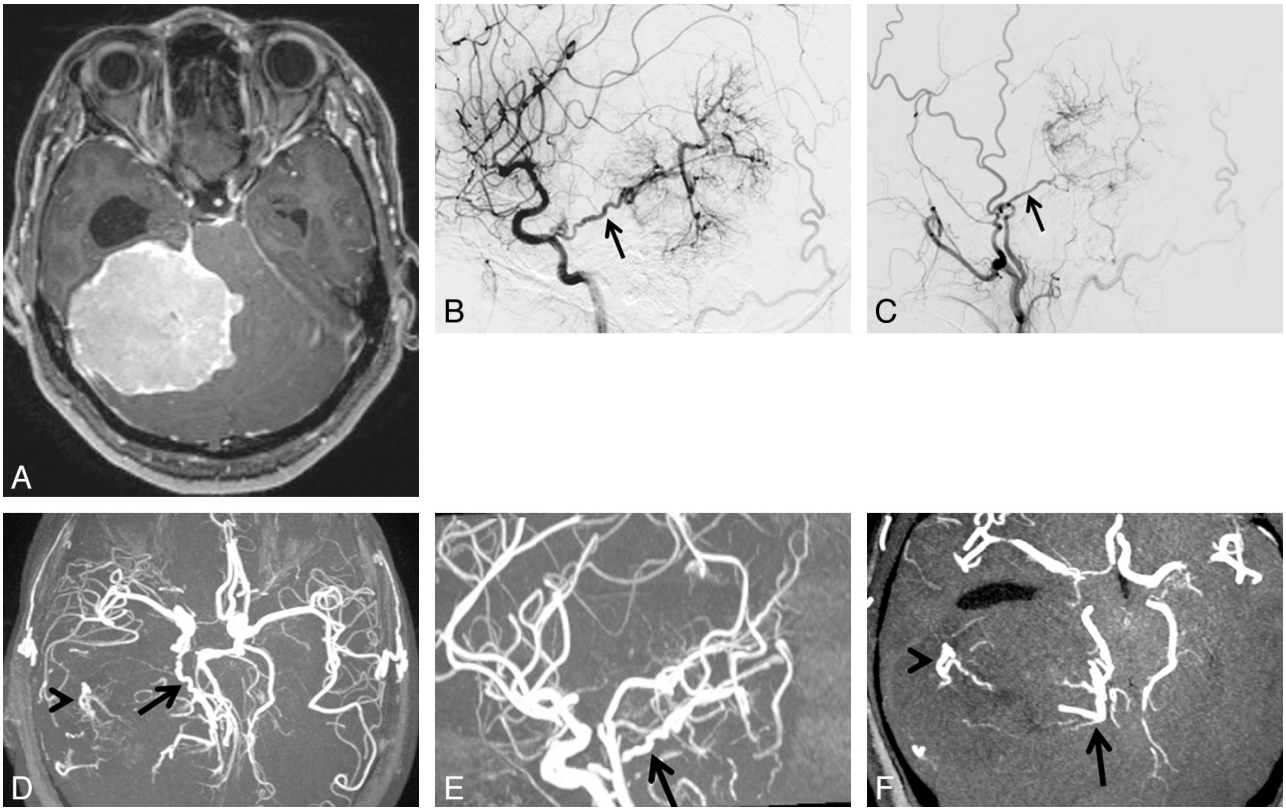

FIG 2. A 49-year-old woman with tentorial meningioma. *A,* Axial contrast-enhanced 3D turbo field echo image showing a large enhanced mass in the supra- to infratentorial regions. *B,* DSA (lateral projection from the right internal carotid artery) reveals a tumor fed primarily by the tentorial artery of the meningohypophyseal trunk (*arrow*). Based on the surgical findings, the dural attachment was the tentorium cerebelli. *C,* DSA (lateral projection from the right external carotid artery) shows a tumor fed partially by the middle meningeal artery (*arrow*). The right middle meningeal artery was judged to be the secondary feeder. *D,* 3D TOF MRA (axial projection) depicts dilated branches from the right tentorial- (*arrow*) and middle meningeal arteries (*arrowhead*). *E,* 3D TOF MRA (sagittal projection) shows the dilated tentorial artery (*arrow*) from the meningohypophyseal trunk of the internal carotid artery. *F,* This axial partial MIP MRA shows tumor-feeding branches from the tentorial artery at the medial portion of the tumor (*arrow*) and from the middle meningeal artery at the lateral portion of the tumor (*arrowhead*). Both readers judged that the tentorial artery of the meningohypophyseal trunk was the primary feeder and that the dural attachment was the tentorium cerebelli.

flow saturation from slow flow. The MOTSA technique minimizes losses in signal intensity caused by spin saturation, maintains small voxels and short TEs to minimize intravoxel phase dispersion,[14,15] and allows larger imaging volumes. Using these techniques we were able to obtain high spatial resolution (reconstructed voxel size 0.25 × 0.25 × 0.5 mm), which allowed the depiction of small arterial feeders.

To evaluate the tumor feeders, our readers used axial source, MIP, and partial MIP MRA, and conventional MR images. Although the MIP algorithm provides angiogram-like images, the lower signal intensity feature of vessels may be lost and small or slow-flowing vessels may not be visualized.[16] MRA source images contain both flow and anatomic information. Small intracranial structures can be seen because the acquisition of submillimeter sections results in high resolution and flow-related enhancement. On partial MIP images, vessels and the surrounding brain in a targeted region of interest can be seen without vessel overlap. To our observers evaluating the feeding arteries, conventional MR images were available, and some feeders could be predicted based on anatomic information provided by conventional MR images. We posit that our display method contributed to the identification of small feeders on 3D TOF MRA images.

Interobserver and intermodality agreements for secondary feeders were slightly lower than for primary feeders. In our study, the spatial resolution of MRA was much lower than that of DSA. Compared with the voxel size of MRA images, the diameter of arterial feeders can be small, and the spatial resolution on these images is not sufficiently high enough to depict them. On unenhanced 3D TOF MRA, the visualization of the feeders (or at least their intensity relative to stationary tissue) will depend on their orientation relative to the scan plane. If the scan plane is parallel to the flowing blood, enhancement may be lost as spins will be exposed to the saturating radio-frequency pulses. In addition, the details of the acquisition parameters (eg, TE, spatial resolution) as well as the vendor-specific details of the pulse sequence may have had an influence on the outcome of our study. Technical advances (eg, 32-channel coils, 7T MR imaging systems) have led to increases in the signal-to-noise ratio[17,18] and may improve the visualization of secondary feeders on MRA images. In 2 of our cases, parasitic or dural branches from the cerebral or cerebellar arteries were not secondary feeders but primary feeders. This unexpected blood supply to the tumor might have affected the readers' interpretation of the MRA images.

The accurate assessment of dural attachments in meningiomas is important for satisfactory surgical outcomes.[3] When the tumors are small or located at a specific area, the dural

Table 3: Interobserver and intermodality agreement for the identification of secondary feeders

	MRA		Interobserver			Intermodality
	Reader 1	Reader 2	Agreement[a]	MRA[b]	DSA	Agreement[c]
MMA	3	2		3	5	
AMA	0	0		0	1	
APhA	1	0		0	1	
OA	0	0		0	1	
OphA	1	2		1	1	
ILT	0	0	15 (71%)	0	0	16 (76%)
MHT	5	3	$\kappa = 0.58$	5	4	$\kappa = 0.72$
ACA	2	2	[0.34–0.82]	2	2	[0.51–0.93]
MCA	2	4		2	2	
PCA	0	0		0	0	
SCA	0	0		0	0	
AICA	0	1		1	0	
PICA	0	0		0	0	
None	7	7		7	4	
Other	0	0		0	0	

Note:—Data are number of meningiomas. Data in parentheses are the percentage of times that results that were concordant, and data in brackets are 95% confidence intervals. MMA indicates middle meningeal artery; AMA, accessory meningeal artery; APhA, ascending pharyngeal artery; OA, occipital artery; OphA, ophthalmic artery; ILT, inferolateral trunk; MHT, meningohypophyseal trunk; MCA, middle cerebral artery; ACA, anterior cerebral artery; PCA, posterior cerebral artery; SCA, superior cerebellar artery; AICA, anterior inferior cerebellar artery; PICA, posterior inferior cerebellar artery.

[a] Agreement of MRA between Reader 1 and Reader 2.

[b] Consensus reading of MRA of Reader 1 and Reader 2.

[c] Agreement between the consensus reading of MRA of Reader 1 and Reader 2 and DSA.

Table 4: Interobserver and intermodality agreement for the location of dural attachment of meningiomas

	MRA/MRI					
	Reader 1	Reader 2	Interobserver Agreement[a]	MRA/MRI[b]	Surgery[c]	Agreement[d]
Convexity	4	4		4	4	
Parasagittal	2	2		2	2	
Falx	1	1		1	1	
Sphenoid ridge	5	6		5	5	
Anterior clinoid	1	0		1	1	
Cen. skull base	1	1	19 (90%)	1	1	21 (100%)
Mid. cran. fossa	1	1	$\kappa = 0.95$	1	1	$\kappa = 1.00$
Tentorial	1	1	[0.84–1.00]	1	1	[1.00–1.00]
Petroclival	2	2		2	2	
T-S junction	1	1		1	1	
CPA	1	1		1	1	
Cerebellar conv.	1	1		1	1	
Other	0	0		0	0	

Note:—Data are number of meningiomas. Data in parentheses are the percentage of times that results that were concordant, and data in brackets are 95% confidence intervals. Cen. skull base indicates central skull base; Mid. cran. fossa, middle cranial fossa; T-S junction, transverse-sigmoid sinus junction; CPA, cerebellopontine angle; Cerebellar conv., cerebellar convexity

[a] Agreement of MRA/MRI between Reader 1 and Reader 2.

[b] Consensus reading of MRA/MRI of Reader 1 and Reader 2.

[c] Final diagnosis of dural attachment was determined by surgical findings. When total tumor resection was not obtained, DSA findings were also used for determining the dural attachment of meningiomas.

[d] Agreement between the consensus reading of MRA/MRI of reader 1 and reader 2 and surgical diagnosis.

attachment site may be easily identified by conventional MR imaging alone. This may not be true for large meningiomas, however. In some earlier reports, the dural attachment of meningiomas was identified, and hyperostosis at the dural attachment site is a phenomenon recognized on CT scans.[19,20] A contrast-enhanced 3D MR technique (eg, fast imaging with steady-state acquisition) may provide information regarding the adhesiveness of dural attachments.[21]Because these are indirect radiologic findings, however, the accurate site at which tumor-feeding arteries enter the tumor via the attached dura mater is not fully understood.

In our study, the addition of 3D TOF MRA to conventional MR imaging was useful for identifying the dural attachment in nearly one-third of the meningiomas, especially large tumors in contact with several areas. We used source and partial MIP images from MRA studies; they contain both anatomic and vessel information at high spatial resolution. We think that this precise information contributed to the identification of the dural attachment with feeding arteries supplying blood to the tumor.

Information on the vessels feeding intracranial hypervascular mass lesions is necessary for a differential diagnosis (eg, intra- versus extra-axial lesions) and for planning interventional procedures.[22] It is also important for surgeons to know the vasculature ahead of time, even without preoperative embolization, to facilitate operative planning. From our study, it is not clear whether MRA appropriately triages patients for beneficial preoperative DSA with or without embolization. The indication of preoperative DSA might be determined by various factors: tumor location, size and vascularity, and feeder location. This information may be obtained from MR imaging and MRA. Further investigations are required to clarify the indication of preoperative DSA. Our results suggest that 3D TOF MRA is useful to identify the feeders of meningiomas. It cannot, however, replace DSA at the planning of interventional procedures because its identification of other feeders is relatively limited. Compared with DSA, 3D TOF MRA also has several disadvantages: lower spatial resolution, the lack of temporal resolution of the vascular flow dynamics, and no information about venous anatomy.

Our study has some limitations. First, it is a preliminary look into a 3D TOF MRA technique at 3T in a specific subset of patients. The temporal and spatial resolution of DSA could be further improved by using smaller FOVs and frame rates of up to 30/s. DSA can also be performed more selectively. Further comparative studies with DSA are needed to clarify the value of this MRA technique. Second, we did not compare unenhanced 3D TOF MRA with contrast-enhanced 3D MRA data. Because contrast-enhanced 3D MRA combines the T1 shortening effect of a gadolinium-based contrast agent, it might yield additional information on the feeding artery.[23] Third, we did not address the actual number of vessels that supplied indi-

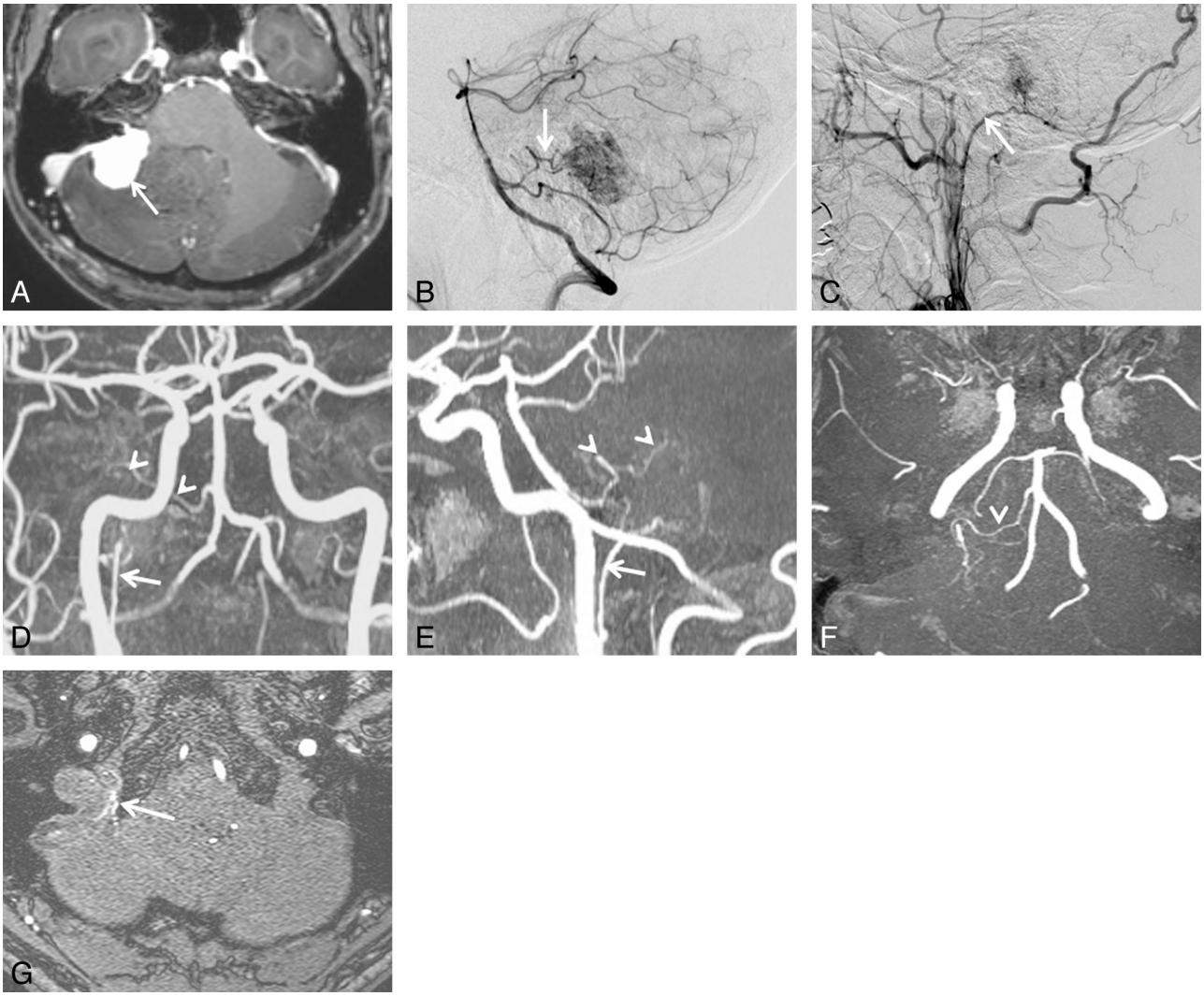

FIG 3. A 49-year-old man with cerebellopontine angle meningioma. *A,* Axial contrast-enhanced 3D turbo field echo image showing an enhanced mass in the cerebellopontine angle region. *B,* DSA (lateral projection from the right vertebral artery) depicts a tumor fed primarily by the anterior inferior cerebellar artery (*arrow*). *C,* DSA (lateral projection from the right external carotid artery) shows a tumor fed partially by the ascending pharyngeal artery (*arrow*). The ascending pharyngeal artery was judged to be the secondary feeder. Based on the surgical findings, the dural attachment was the cerebellopontine angle. On the 3D TOF MRA image (anteroposterior projection) (*D*) and sagittal partial MIP-MRA image (*E*), the right ascending pharyngeal (*arrow*) and anterior inferior cerebellar artery (*arrowheads*) are well visualized. *F,* Axial partial MIP-MRA image showing tumor-feeding branches from the right anterior inferior cerebellar artery (*arrowhead*). *G,* Axial source MRA image showing tumor-feeding jugular branches from the right ascending pharyngeal artery (*arrow*). One reader judged that the anterior inferior cerebellar artery was the primary feeder and that the ascending pharyngeal artery was the secondary feeder. The other reader came to the opposite conclusion. Both readers concluded that the dural attachment was the cerebellopontine angle.

vidual tumors. Fourth, our data were obtained from a single-center study in a small number of patients. Additional studies with large populations are needed.

CONCLUSIONS

The excellent agreement between MRA and DSA findings suggests that unenhanced MRA at 3T is a reliable diagnostic tool for the identification of the primary meningioma feeders. MRA at 3T, however, cannot at present replace DSA for the identification of the feeding arteries of intracranial meningiomas. The combined information from MRA and conventional MR imaging may be useful for evaluating the dural attachment of meningiomas.

REFERENCES

1. Wiemels J, Wrensch M, Claus EB. **Epidemiology and etiology of meningioma.** *J Neurooncol* 2010;99:307–14
2. Gemmete JJ, Ansari SA, McHugh J, et al. **Embolization of vascular tumors of the head and neck.** *Neuroimaging Clin N Am* 2009;19:181–98
3. Adachi K, Kawase T, Yoshida K, et al. **ABC surgical risk scale for skull base meningioma: a new scoring system for predicting the extent of tumor removal and neurological outcome.** *J Neurosurg* 2009;111:1053–61
4. Bassiouni H, Asgari S, Sandalcioglu IE, et al. **Anterior clinoidal meningiomas: functional outcome after microsurgical resection in a consecutive series of 106 patients.** *J Neurosurg* 2009;111:1078–90
5. Hu WY, TerBrugge KG. **The role of angiography in the evaluation of vascular and neoplastic disease in the external carotid artery circulation.** *Neuroimaging Clin N Am* 1996;6:625–44

6. Du C, Korogi Y, Nagahiro S, et al. **Hemifacial spasm: three-dimensional MR images in the evaluation of neurovascular compression.** *Radiology* 1995;197:227–31
7. Hirai T, Korogi Y, Hamatake S, et al. **Three-dimensional FISP imaging in the evaluation of carotid cavernous fistula: comparison with contrast-enhanced CT and spin-echo MR.** *AJNR Am J Neuroradiol* 1998;19:253–59
8. Willinek WA, Born M, Simon B, et al. **Time-of-flight MR angiography: comparison of 3.0-T imaging and 1.5-T imaging–initial experience.** *Radiology* 2003;229:913–20
9. Schmitz BL, Aschoff AJ, Hoffmann MH, et al. **Advantages and pitfalls in 3T MR brain imaging: a pictorial review.** *AJNR Am J Neuroradiol* 2005;26:2229–37
10. DeLano MC, DeMarco JK. **3.0 T versus 1.5 T MR angiography of the head and neck.** *Neuroimaging Clin N Am* 2006;16:321–41
11. Kunii N, Ota T, Kin T, et al. **Angiographic classification of tumor attachment of meningiomas at the cerebellopontine angle.** *World Neurosurg* 2011;75:114–21
12. Kadota T, Kuriyama K, Inoue E, et al. **MR angiography of meningioma.** *Magn Reson Imaging* 1993;11:473–83
13. Engelhard HH. **Progress in the diagnosis and treatment of patients with meningiomas. Part I: diagnostic imaging, preoperative embolization.** *Surg Neurol* 2001;55:89–101
14. Blatter DD, Parker DL, Robison RO. **Cerebral MR angiography with multiple overlapping thin slab acquisition. Part I. Quantitative analysis of vessel visibility.** *Radiology* 1991;179:805–11
15. Davis WL, Blatter DD, Harnsberger HR, et al. **Intracranial MR angiography: comparison of single-volume three-dimensional time-of-flight and multiple overlapping thin slab acquisition techniques.** *AJR Am J Roentgenol* 1994;163:915–20
16. Tsuruda J, Saloner D, Norman D. **Artifacts associated with MR neuroangiography.** *AJNR Am J Neuroradiol* 1992;13:1411–22
17. Parikh PT, Sandhu GS, Blackham KA, et al. **Evaluation of image quality of a 32-channel versus a 12-channel head coil at 1.5T for MR imaging of the brain.** *AJNR Am J Neuroradiol* 2011;32:365–73
18. von Morze C, Xu D, Purcell DD, et al. **Intracranial time-of-flight MR angiography at 7T with comparison to 3T.** *J Magn Reson Imaging* 2007;26:900–04
19. Akutsu H, Sugita K, Sonobe M, et al. **Parasagittal meningioma en plaque with extracranial extension presenting diffuse massive hyperostosis of the skull.** *Surg Neurol* 2004;61:165–69
20. Bikmaz K, Mrak R, Al-Mefty O. **Management of bone-invasive, hyperostotic sphenoid wing meningiomas.** *J Neurosurg* 2007;107:905–12
21. Yamamoto J, Kakeda SH, Takahashi M, et al. **Dural attachment of intracranial meningiomas: evaluation with contrast-enhanced three-dimensional fast imaging with steady-state acquisition (FIESTA) at 3T.** *Neuroradiology* 2010;53:413–23
22. Latchaw RE. **Preoperative intracranial meningioma embolization: technical considerations affecting the risk-to-benefit ratio.** *AJNR Am J Neuroradiol* 1993;14:583–86
23. Reinacher P, Reinges MH, Simon VA, et al. **Dynamic 3-D contrast-enhanced angiography of cerebral tumours and vascular malformations.** *Eur Radiol* 17 Suppl 6 2007:F52–62